

A 3-D Indoor Analysis of Path Loss Modeling Using Kriging Techniques

Melissa Diago-Mosquera [✉], Alejandro Aragón-Zavala [✉], *Senior Member, IEEE*,
Leyre Azpilicueta [✉], *Senior Member, IEEE*, Raed Shubair [✉], *Senior Member, IEEE*,
and Francisco Falcone [✉], *Senior Member, IEEE*

Abstract—This study proposes a novel measurement-based method to predict and model three-dimensional (3-D) path loss in indoor scenarios, which first regresses 28 GHz measurements via median path loss modeling and then includes ordinary Kriging to interpolate shadowing. The performance of this method is evaluated by investigating the spatial structure that follows shadowing through the semivariogram, covariance function, and correlogram as variography tools. It is shown that semivariogram outperforms the other statistics to describe shadowing spatial continuity in path loss modeling in terms of the mean absolute error.

Index Terms—Indoor path loss model, Kriging, three-dimensional (3-D), variography.

I. INTRODUCTION

TO QUANTIFY the reliability of coverage provided by any base station, it is essential to understand and characterize radio propagation factors, which consist of median path loss and shadowing as the main path loss components for indoor scenarios. When rigorous fit design and reliable predictions are the principal approaches, hybrid path loss models are the best method for estimating and analyzing radio propagation. Usually, in these models, measurement datasets are first regressed via linear median path loss modeling and then shadowing is generated as random variable. For accurate predictions in in-building modeling it is necessary to consider the variability of the signal path due to obstacles and scenario geometry. Therefore, shadowing should be predicted considering the singularities associated with the evaluated scenario.

Kriging is a powerful technique for this constraint, this analytical solution provides clear steps to go through when estimating unknown values at unmeasured locations. Besides, prior to the

interpolation to predict unmeasured from measured values, this technique employs variography to explore the spatial structure of the variable under study, in this case, to provide a suitable description of the dispersion with respect to the nominal value given by the in-building path loss model.

A. Related Works

In hybrid models, specifically measurement-based, measurement campaigns are carried out to gain a better understanding of path loss behavior, allowing an accurate fitting of the specific scenario. Kriging, as a geostatistical technique, takes advantage of these measurements to predict values at unmeasured locations forming weights from surrounding known measured values, considering that the closest samples have the most influence. By looking at the spatial structure of the samples, it is possible to calculate Kriging weights. This process is named variography and its main goal is to explore the spatial dependence in order to quantify it through a fitted model, which can be obtained by plotting the semivariogram, covariance, or correlogram.

Recent works in radio propagation have employed Kriging to interpolate path loss [1], shadowing [2]–[6], and received power [7], [8] as part of the modeling process. All these studies have been performed in two-dimensions and employed the semivariogram as part of the variography stage, however, none of these studies explain or justify such a choice. In consequence, it is necessary to address and understand if the semivariogram is the best choice to investigate graphically the spatial patterns of the samples.

B. Our Contributions

The aim of this study is encouraged by the need to provide and validate an accurate method to estimate three-dimensional (3-D) path loss in indoor scenarios including Kriging as a geostatistical technique to predict the shadowing component. Therefore, the main contributions are summarized as follows.

- 1) From a complete analysis of the variography process, it is demonstrated that the semivariogram outperforms the other statistics to describe shadowing spatial continuity in path loss modeling.
- 2) To achieve accurate predictions, Kriging strongly depends on the use of a suitable fitted model, which is provided by the variography results. Through the first contribution, the best performance of Kriging is guaranteed. Then, it is employed to predict shadowing to estimate the path loss in a 3-D indoor scenario. We validate the accuracy of the

Manuscript received March 2, 2022; accepted March 19, 2022. Date of publication March 24, 2022; date of current version June 2, 2022. This work was supported by the National Council of Science and Technology CONACYT, through the student scholarship number 746015, under Project RTI2018-095499-B-C31, funded by the Ministerio de Ciencia, Innovación y Universidades, Gobierno de España (MCIU/AEI/FEDER, UE). (*Corresponding author: Leyre Azpilicueta.*)

Melissa Diago-Mosquera and Alejandro Aragón-Zavala are with the Escuela de Ingeniería y Ciencias, Tecnológico de Monterrey, Querétaro 76130, Mexico (e-mail: a00829220@itesm.mx; aaragon@tec.mx).

Leyre Azpilicueta is with the Escuela de Ingeniería y Ciencias, Tecnológico de Monterrey, Monterrey 64849, Mexico (e-mail: leyre.azpilicueta@tec.mx).

Raed Shubair is with the Department of Electrical and Computer Engineering, New York University Abu Dhabi, Abu Dhabi 129188, UAE (e-mail: raed.shubair@nyu.edu).

Francisco Falcone is with the Department of Electric, Electronic and Communication Engineering and the Institute of Smart Cities, Public University of Navarre, 31006 Pamplona, Spain (e-mail: francisco.falcone@unavarra.es).

Digital Object Identifier 10.1109/LAWP.2022.3162160



Fig. 1. Indoor scenario within the library building at TEC Monterrey, employed for the measurement campaign.

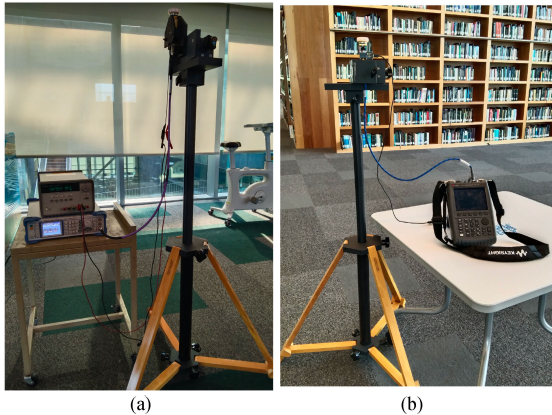


Fig. 2. Measurement equipment. (a) Transmitter. (b) Receiver.

methodology by comparing the results against measured data.

II. EXPERIMENTAL MEASUREMENT DESCRIPTION

A. Measurement Environment

To perform feasible in-building radio propagation modeling to proceed with confidence to the path loss predictions, radio measurements were carried out at 28 GHz in the 4th floor of the library of Tecnológico de Monterrey, campus Monterrey, as is illustrated in Fig. 1. This floor of the library is an open room that has three wooden bookcases evenly distributed in the target area, with exterior walls built with metallic beams and glass. Ceilings are built with drywall while the floor with concrete covered by a carpet material. This indoor scenario enables to carry out both line-of-sight and non-line-of-sight measurements. The transmitter system was located at a 1.5 m height and the receiver at 1 and 2 m heights. The measurement campaign was planned to collect samples on a grid (42 m long and 12 m wide) with squares of 2 m on each side, where the transmitter was located at the center of the grid at the low end. This setting yields 132 samples for each receiver height and a total of 264 measurements.

B. Measurement Equipment

To collect received power samples in the selected scenario, a complete radio propagation system was deployed, as is illustrated in Fig. 2. The transmitter system consisted of a Rohde & Schwarz microwave signal generator, model SMB100A, set at an operating frequency of 14 GHz. To access the frequency of 28 GHz, an up-converter (Farran Technologies, model FDA-K/28) with a multiplication factor of 2 was employed. It was

connected to an omnidirectional vertically polarized antenna with 3 dBi gain, G_{TX} , model SAO-2734030345-KF-S1. The transmitter power P_{TX} was 24 dBm.

The receiver system was composed of a vertically polarized omnidirectional antenna equipped with a low noise amplifier (LNA), model SAO-2734033045-KF-C1-BL, with 30 dB of receiver gain G_{RX} , of which 3 dBi were from the antenna and 27 dB from the integrated LNA. The receiver was plugged into a Keysight Field Fox N9952A microwave spectrum analyzer.

III. 3-D PATH LOSS MODELING

A. Path Loss Extraction

From the resulting power received measurements and considering the link budget of the radio propagation system, the path loss of the links is calculated in dB as follows:

$$L = P_{TX} + G_{TX} + G_{RX} - P_{RX} \quad (1)$$

where P_{TX} is the transmitted power, G_{TX} and G_{RX} the antenna gains employed to transmit and receive, respectively, and P_{RX} the measured power.

In the validation process it is necessary to quantify how well the model predicts the path loss at specific locations, locations which are obtained from testing dataset. Therefore, the path loss extracted is grouped into tuning and testing datasets. This process is based on radial sectors, where samples are extracted from each sector keeping a 60/40 rate, 60% for tuning and 40% for testing, following the methodology described in [5].

B. Model Tuning

For modeling median path loss L_{50} , it is considered the simplest form of power law model

$$L_{50} = 10n \log d + e \quad (2)$$

where d is the Euclidean distance between the transmitter and the receiver antenna, which have a 3-D coordinate system to represent their location in the target area. The path loss exponent n and the path loss intercept e are tuned with the tuning dataset of the path loss measurements extracted in (1), in order to adjust the model with specific characteristics and site details considered in the radio measurements carried out.

C. Shadowing Extraction and Generation

The path loss also depends on the shadowing L_s , which is the result of the sum between L_{50} and L_s . Therefore, it is possible to extract the shadowing component as follows:

$$L_s = L - L_{50}. \quad (3)$$

To predict and quantify the shadowing component in specific locations, ordinary Kriging is employed. Through this geostatistical technique, Kriging weights are generated for the known shadowing values to employ it to calculate a shadowing prediction for the location with the unknown value. To proceed, first, the spatial structure of (3) must be explored by variography in order to provide reliable Kriging weights.

IV. VARIOGRAPHY AND KRIGING INTERPOLATION

To investigate and quantify the spatial structure, empirical tools such as semivariogram, covariance function, and correlogram can be employed.

A. Variography: Spatial Modeling

The empirical semivariogram is computed as follows:

$$\gamma(h) = \frac{1}{2N(h)} \sum_{i=1}^{N(h)} (z_i - z_{i+h})^2 \quad (4)$$

where $N(h)$ is the number of pairs within the lag interval h , z_i is the known value at 3-D location i , and z_{i+h} is another known value separated by a lag h from i . In other words, h is a vector that represents the separation distance between two spatial locations.

The empirical covariance is calculated as follows:

$$C(h) = \frac{1}{N(h)} \sum_{i=1}^{N(h)} z_i \cdot z_{i+h} - m_i \cdot m_{i+h} \quad (5)$$

where m_i and m_{i+h} are given by the following:

$$m_i = \frac{1}{N(h)} \sum_{i=1}^{N(h)} z_i, \quad m_{i+h} = \frac{1}{N(h)} \sum_{i=1}^{N(h)} z_{i+h}. \quad (6)$$

And the empirical correlation is computed as follows:

$$\rho(h) = \frac{C(h)}{\sqrt{\sigma_i + \sigma_{i+h}}} \quad (7)$$

where σ_i and σ_{i+h} are given by the following:

$$\begin{aligned} \sigma_i &= \frac{1}{N(h)} \sum_{i=1}^{N(h)} (z_i - m_i)^2, \quad \sigma_{i+h} \\ &= \frac{1}{N(h)} \sum_{i=1}^{N(h)} (z_{i+h} - m_{i+h})^2. \end{aligned} \quad (8)$$

When the empirical functions (4), (5), and (7) are graphed versus the lag distance h , the semivariogram, the covariance function, and the correlogram tools are obtained. These tools provide information about the spatial correlation of the known data; however, all possible distances are not covered by the empirical functions, therefore, it is necessary to fit a theoretical model, which is what is actually used to develop the Kriging weights. This model must be a continuous function to guarantee positive Kriging variances.

Considering the accuracy of the results assessed for path loss modeling in [5], the exponential function is selected to provide a semivariogram fitting. Consequently, the semivariogram model is expressed as follows:

$$\gamma_{\text{exp}}(h) = s \cdot \left(1 - e^{-3h/r}\right) \quad (9)$$

where s is the sill, the semivariance value at which the semivariogram yields a plateau, and r is the range, the separation distance at which the semivariogram reaches s .

If the spatial dependency of the measured known values is analyzed by employing the covariance function, the fitting model, resulting from the variography, is calculated considering that the covariance function obeys the following relationship:

$$C(h) = \sigma^2 - \gamma_{\text{exp}}(h) \quad (10)$$

where σ^2 is the variance of the variable under consideration z , and $\gamma_{\text{exp}}(h)$ is the exponential function described in (9).

Therefore, the fitting model when covariance function tool is selected is as follows:

$$C_{\text{exp}}(h) = s \cdot e^{-3h/r}. \quad (11)$$

Similarly, when the correlogram tool is employed, it obeys the following relationship:

$$\rho(h) = \frac{C(h)}{\sigma^2} \quad (12)$$

where $C(h)$ is the function described in (11). Once the corresponding values are replaced in (12) the fitting model is calculated as follows:

$$\rho_{\text{exp}}(h) = e^{-3h/r}. \quad (13)$$

At this point, it is clear that there are three options of statistical tools for modeling the spatial patterns of measured samples through a fitted model $f(h)$ computed by (9), (11), or (13), depending on the tool selection, where s and r are calculated by fitting a least-squares regression analysis to the empirical values.

Going on the variography, the binning process is adopted for spatial modeling. Over this process, properly neighbor samples, as described in [5], will restrict how far and where to look for the samples to be used in the prediction, for this process a distance separation matrix between all measured locations is created as D . Toward selecting a suitable lag h and placing a maximum lag limit on the calculation of (4), (5), and (7), it is important to understand this process. Since the estimated values in the variography tend to become more erratic with increasing distances, boundaries are necessary to analyze D . The maximum lag limit is the maximum distance that is going to be considered and is calculated as the half of the maximum distances reported in D , while h determines the lag interval considered to find measured neighbors, which is calculated as the mean of the minimum distance extracted from D . For instance, $z_i - z_{i+h}$ in (4), is grouped based on their corresponding lag interval h —resulting in $N(h)$ pairs—up to the maximum lag to calculate (4) for each separation distance reported in D .

B. Ordinary Kriging for Shadowing Generation

Then, when the spatial patterns have been modeled by fitting a theoretical function $f(h)$, ordinary Kriging employs it to interpolate known data and predict values at unsampled locations by solving the following equation:

$$k = V^{-1} \cdot v \quad (14)$$

where the matrix V is composed by the values resulting from $f(h)$ with h as the distances between the pairs of measured points, the vector v contains the result of compute the distance of each measured locations to the prediction location and substituting it as the lag h in $f(h)$, and k is composed by the Kriging weights λ_i and the Lagrange multiplier l .

When calculating (14) the weights are found and the predicted value \hat{z}_0 at unmeasured place is provided by the following:

$$\hat{z}_0 = \sum_{i=1}^{N(h)} \lambda_i \cdot z_i. \quad (15)$$

Fig. 3 shows an example of shadowing-aided predictions employed by the variography tools when a random 60/40 is selected (considering the radial grouping process). In Fig. 3,

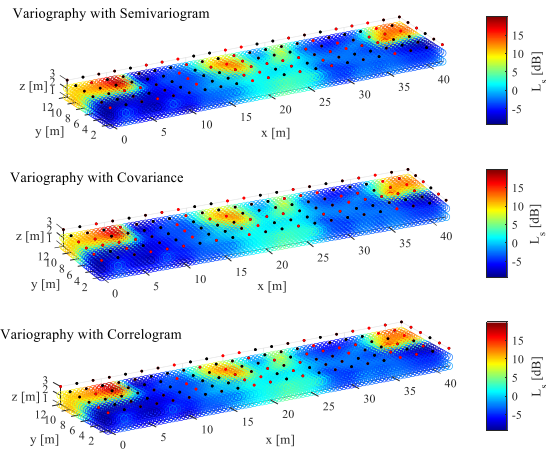


Fig. 3. Shadowing prediction results obtained by variography analysis.

TABLE I
PATH LOSS PREDICTIONS PERFORMANCE

Tool	$\gamma(h)$	$C(h)$	$\rho(h)$
MAE	2.70	2.81	2.72

tuning and testing dataset locations are plotted with black and red dots, respectively.

V. 3-D PATH LOSS PREDICTIONS

For 3-D indoor path loss predictions, particular data features are required, considering the aim of aided-shadowing Kriging, the variable z described in Section IV corresponds to the shadowing for the tuning dataset extracted in (3) from the measurements. Thus, to predict path loss at specific location in the 3-D indoor space, the next model is followed:

$$\hat{L} = 10n \log d + e + \sum_{i=1}^{N(h)} \lambda_i \cdot L_{si}. \quad (16)$$

One of the aims of this study is encouraged by the fact that on the performance of feasible and accurate Kriging interpolation processing, there is no explicit research to understand and correctly select the best statistical tool to be employed in the preliminary variography process. For this reason, the performance of the variogram, the covariance function and the correlogram is analyzed by comparing the predicted path loss values \hat{L}_i with the measured path loss L_i at the remaining test locations t_N , in terms of the mean absolute error (MAE), which is given by the following:

$$\text{MAE} = \frac{1}{t_N} \sum_{i=1}^{t_N} |L_i - \hat{L}_i|. \quad (17)$$

For a reliable analysis, 1000 iterations are assessed to extract different 60/40 groups for tuning and testing dataset through the radial algorithm described for the path loss extraction. Each value presented in Table I is obtained as the 1000-result average for each statistical tool employed in the variography process.

Furthermore, once the 1000-samples are performed the results of the Kriging-aided model is presented for the tools analyzed

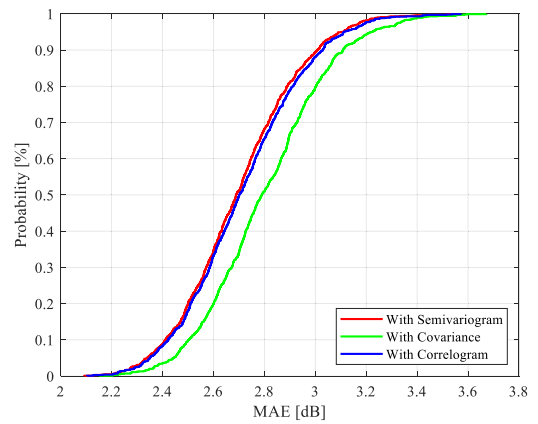


Fig. 4. CDFs of MAE over path loss predictions based on the three tools.

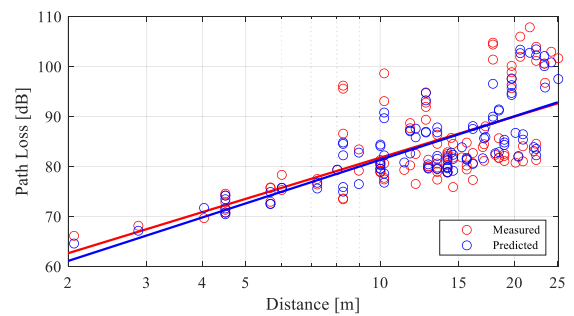


Fig. 5. Path loss prediction versus measurement results for the testing dataset.

in terms of the cumulative distribution function (CDF) for the MAE in Fig. 4.

According to Table I and Fig. 4, it can be seen that employing semivariogram and correlogram for shadowing spatial modeling improves the accuracy of Kriging at 28 GHz. With an MAE of 2.7 dB, the semivariogram guarantees the high level of confidence of the spatial modeling, thus, when it is employed, the proposed model achieves accurate path loss indoor predictions at 28 GHz. However, even though the covariance function has the highest MAE, it is still a small error of 2.81 dB for indoor path loss predictions compared to other hybrid models available in the literature [9].

Considering the profitable results when semivariogram is employed as a statistical tool for variography process in shadowing predictions, Fig. 5 shows the predicted path loss with the model here described and the path loss extracted from measurements at the testing locations, as well as the fitting lines for each case.

VI. CONCLUSION

The aim of this study seeks to evaluate the performance of the specific tool used in variography as part of the Kriging-aided shadowing predictions for indoor path loss modeling. Specifically, we focused on whether the choice of semivariogram, covariance function or correlogram as a statistical tool influences the improvement of the path loss estimation accuracy. The novel knowledge obtained through this work is that in an indoor scenario, correlogram achieves an almost equal performance of semivariogram, even though semivariogram is validated as the most accurate tool to describe shadowing spatial continuity in enclosed spaces for 3-D path loss modeling at 28 GHz.

REFERENCES

- [1] N. Faruk *et al.*, "Path loss predictions in the VHF and UHF bands within urban environments: Experimental investigation of empirical, heuristics and geospatial models," *IEEE Access*, vol. 7, pp. 77293–77307, 2019.
- [2] K. Sato, K. Inage, and T. Fujii, "Radio environment map construction with joint space-frequency interpolation," in *Proc. Int. Conf. Artif. Intell. Inf. Commun.*, Feb. 2020, pp. 051–054, doi: [10.1109/ICAII48513.2020.9065217](https://doi.org/10.1109/ICAII48513.2020.9065217).
- [3] K. Sato, K. Inage, and T. Fujii, "On the performance of neural network residual Kriging in radio environment mapping," *IEEE Access*, vol. 7, pp. 94557–94568, 2019.
- [4] M. E. Diago-Mosquera, A. Aragon-Zavala, F. A. Rodriguez-Corbo, M. Celaya-Echarri, R. Shubair, and L. Azpilicueta, "Tuning selection impact on Kriging-aided in-building path loss modeling," *IEEE Antennas Wireless Propag. Lett.*, vol. 21, no. 1, pp. 84–88, Jan. 2022, doi: [10.1109/LAWP.2021.3118673](https://doi.org/10.1109/LAWP.2021.3118673).
- [5] M. E. Diago-Mosquera, A. Aragón-Zavala, and C. Vargas-Rosales, "The performance of in-building measurement-based path loss modelling using Kriging," *Microw. Antennas Propag.*, vol. 15, no. 12, pp. 1564–1576, 2021, doi: [10.1049/mia2.12163](https://doi.org/10.1049/mia2.12163).
- [6] M. E. Diago-Mosquera, A. Aragón-Zavala, and M. Rodriguez, "Testing a 5G communication system: Kriging-aided O2I path loss modeling based on 3.5 GHz measurement analysis," *Sensors*, vol. 21, no. 20, Oct. 2021, Art. no. 6716, doi: [10.3390/S21206716](https://doi.org/10.3390/S21206716).
- [7] N. Mezhoud, M. Oussalah, A. Zaatri, and Z. Hammoudi, "Hybrid Kriging and multilayer perceptron neural network technique for coverage prediction in cellular networks," *Int. J. Parallel, Emergent Distrib. Syst.*, vol. 35, no. 6, pp. 682–706, Nov. 2020, doi: [10.1080/17445760.2020.1805609](https://doi.org/10.1080/17445760.2020.1805609).
- [8] K. Sato, K. Inage, and T. Fujii, "Modeling the Kriging-aided spatial spectrum sharing over log-normal channels," *IEEE Wireless Commun. Lett.*, vol. 8, no. 3, pp. 749–752, Jun. 2019.
- [9] M. E. Diago-Mosquera, A. Aragon-Zavala, and G. A. Castanon, "Bringing it indoors: A review of narrowband radio propagation modeling for enclosed spaces," *IEEE Access*, vol. 8, pp. 103875–103899, 2020.